Magnetic phase diagram, static properties, and relaxation of the insulating spin glass $Co_{1-x}Mn_xCl_2 \cdot 2H_2O$

G. C. DeFotis, D. S. Mantus, E. M. McGhee, K. R. Echols, and R. S. Wiese
Chemistry Department, College of William and Mary, Williamsburg, Virginia 23185
(Received 29 January 1988)

The magnetic behavior of $Co_{1-x}Mn_xCl_2 \cdot 2H_2O$ has been studied by dc magnetization and susceptibility measurements on a wide range of compositions. This system is a mixture of two isomorphous three-dimensional antiferromagnets of different magnetic periodicity, in which random competing short-range antiferromagnetic and ferromagnetic exchange interactions occur. Spin-glass behavior is observed and examined in several ways. In general, a particular composition exhibits a higher temperature transition to an essentially antiferromagnetic state and a second lower temperature transition to a spin-glass state, or perhaps a mixed spin-glass–antiferromagnetic state. The upper transition temperature is strongly composition dependent, while the lower, at 2.50 ± 0.10 K, is virtually independent of composition. An $x = 0.452$ mixture, in which hysteretic and time-dependent effects are especially strong, is studied in detail. Substantial nonlinearity in its magnetization is observed, and the derived nonlinear susceptibility suggests that a phase transition occurs near 2.45 K. The thermoremanent magnetization (TRM) and isothermal remanent magnetization are also studied and exhibit features characteristic of spin glasses. The temperature dependence of the TRM is reminiscent of that in certain other insulating spin glasses, but does not seem to follow any simple functional form. The time dependence of the TRM is also studied in some detail. Of several theoretical decay expressions tested, the most satisfactory appears to be a stretched exponential with a power-law prefactor. The T-vs-x magnetic phase diagram appears to be of a qualitatively new type, though comparison with other systems can also be made.

I. INTRODUCTION

Quite a number of examples have been studied in which the competing orthogonal spin anisotropies of two isomorphous insulating magnetic systems containing different metal ions leads to multicritical point structure in the magnetic phase diagram of the mixed system. A particularly well-studied case is $Fe_{1-x}Co_xCl_2$.[1,2] Also of great interest are mixed systems in which, though the spin anisotropies may not be orthogonal, various other types of competing interactions are present. In such cases spin-glass phases can occur.[3] It is convenient to distinguish between two classes of such systems: (1) those in which strongly competing ferromagnetic and antiferromagnetic interactions occur, with consequent frustration, and (2) those in which predominantly antiferromagnetic interactions occur, but with a balance such that significant frustration again arises. In the first class, dilute ferromagnets like $Eu_xSr_{1-x}S$ are the systems in which spin-glass behavior is most frequently observed.[4] Here the effects of a weaker antiferromagnetic next-nearest-neighbor interaction, already present in the pure system, are enhanced by the randomness associated with dilution. A mixture of a ferromagnet and an antiferromagnet exhibiting spin-glass behavior has been much less frequently realized. The best example is probably $Rb_2Mn_{1-x}Cr_xCl_4$.[5] In the second class of systems, more readily prepared since isomorphous series of transition metal compounds tend to contain mostly antiferromagnets, spin-glass behavior has again much more frequently been observed in dilute systems, such as $ZnCr_{2x}Ga_{2-2x}O_4$.[6] The mixing of two isomorphous antiferromagnets generally has not led to the formation of a spin glass, presumably because in most cases the degree of frustration (which can already be present in either or both pure systems) has not been sufficiently enhanced by the mixing. However, $Fe_xMn_{1-x}TiO_3$ is one recently discovered example of this type.[7]

We recently studied the mixed magnetic insulator $Fe_{1-x}Mn_xCl_2 \cdot 2H_2O$.[8] Each of the pure components orders antiferromagnetically, but while $MnCl_2 \cdot 2H_2O$ has only antiferromagnetic interactions ($J_1/k = -0.45$ K along $\cdots MCl_2MCl_2M \cdots$ chemical chains, and $J_2/k = -0.48$ K between the chains),[9] pure $FeCl_2 \cdot 2H_2O$ has both ferromagnetic and antiferromagnetic interactions ($J_1/k = 0.84$ K along chains and $J_2/k = -0.40$ K between chains).[10] The T-x magnetic phase diagram contained both an apparent tetracritical point (the spin anisotropies of the Fe and Mn ions are orthogonal) and spin-glass regions. The latter were attributed to the presence of competing ferromagnetic and antiferromagnetic interactions of comparable strength in the mixture. Spin-glass behavior was generally more pronounced on the Mn-rich side of the phase diagram, due presumably to the rather stronger intrachain exchange in $FeCl_2 \cdot 2H_2O$ than in $MnCl_2 \cdot 2H_2O$. That is, relatively less iron is favorable with respect to obtaining an appropriate balance (high frustration) of net ferromagnetic and antiferromagnetic interaction strengths; above about 55% iron the stronger ferromagnetic interaction of this com-

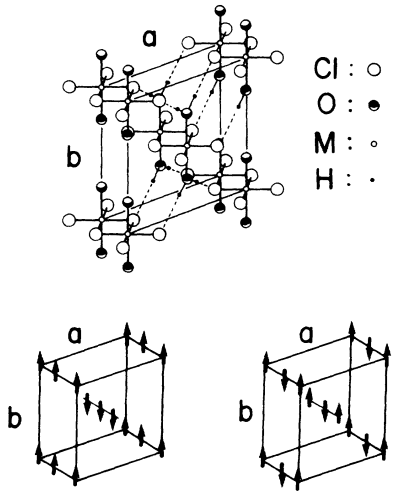

FIG. 1. Upper part: common crystal structure of $CoCl_2 \cdot 2H_2O$ and $MnCl_2 \cdot 2H_2O$. Lower left: ordered spin arrangement in $CoCl_2 \cdot 2H_2O$. Lower right: ordered spin arrangement in $MnCl_2 \cdot 2H_2O$.

ponent appears to dominate sufficiently to make spin-glass behavior unobservable.

In this paper we examine a closely related mixed magnetic system, $Co_{1-x}Mn_xCl_2 \cdot 2H_2O$. As in the case of $Fe_{1-x}Mn_xCl_2 \cdot 2H_2O$, the pure components are isomorphous monoclinic three-dimensional antiferromagnets, with lattice constants differing by only a few percent. The Co system is much more anisotropic[11,12] and can be described as Ising-like, while the Mn system is nearly isotropic[9] and Heisenberg-like. However, the ordered spin arrangements are colinear (along the twofold b axis), so that in contrast to the Fe-Mn mixture, competing orthogonal spin anisotropies are absent; see Fig. 1. As with $Fe_{1-x}Mn_xCl_2 \cdot 2H_2O$ however, the components of $Co_{1-x}Mn_xCl_2 \cdot 2H_2O$ differ in two ways: (1) while the Mn system contains only antiferromagnetic interactions, the Co system contains both ferromagnetic and antiferromagnetic interactions ($J_1/k = 1.1$ K along $\cdots MCl_2MCl_2M \cdots$ chains and $J_2/k = -0.52$ K between chains),[10,12] and (2) the ordered spin arrangements are such that the two components differ in magnetic periodicity, the magnetic unit cell being the same size as the chemical unit cell in $CoCl_2 \cdot 2H_2O$, but twice as large in $MnCl_2 \cdot 2H_2O$. Substantial frustration should be present in the mixed system therefore, and spin-glass behavior can be anticipated. This is indeed observed, and the structure of the T-x magnetic phase diagram appears to be of a new type.

II. EXPERIMENTAL

Aqueous solutions of $CoCl_2 \cdot 6H_2O$ and $MnCl_2 \cdot 4H_2O$ in desired proportions were prepared and evaporated to dryness at 80 °C, thus ensuring formation of the dihydrate. The material collected was violet and polycrystalline. Commercial chemical analysis confirmed the hydration state and general composition of the materials. Co and Mn concentrations were determined by atomic absorption spectrometry and were generally within 0.01 mole fraction unit of the nominal composition. Analysis of different portions of material from one particular batch gave compositions agreeing to within 0.005 mole fraction unit, about the experimental uncertainty. X-ray diffraction patterns indicated that samples were microscopically homogeneous at the level probed by this technique, and showed that any uptake of water on short exposure to air prior to measurement did not lead to significant formation of higher hydrates. Diffraction peak positions suggested that lattice spacings in several mixtures were intermediate between those of the pure constituents.

Magnetization and susceptibility measurements were made using a variable temperature vibrating sample magnetometer system described previously.[13] Except where otherwise indicated, susceptibility data presented here are field-cooled measurements, with a (rather small) demagnetization correction applied. Such data are believed to be accurate to ± 2–3%, with a precision much better than this. Temperatures, measured with a carbon-glass resistance thermometer located in immediate proximity to the samples, are estimated to be accurate to ± 0.005–0.02 K, depending on the range. Magnetic field values are accurate to $\pm$max(2 G, 0.1%). For zero-field cooling experiments, an external power supply was used to cancel the residual field of the electromagnet; the applied field in this case is believed to be 0 ± 0.5 G.

III. RESULTS AND ANALYSIS

A. Susceptibility and magnetization

Inverse molar susceptibilities as a function of temperature for a series of polycrystalline samples of $Co_{1-x}Mn_xCl_2 \cdot 2H_2O$ are shown in Fig. 2. Above about 20 K all data are linear, with antiferromagnetic deviations appearing at lower temperatures. $\chi_M = C/(T - \Theta)$ fits to the data in the linear regime reveal a fairly regular variation in the effective Curie constant with composition, between the values for $CoCl_2 \cdot 2H_2O$ and

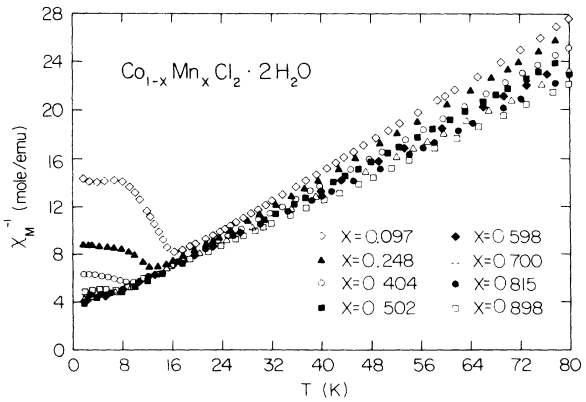

FIG. 2. Inverse molar magnetic susceptibility vs temperature for different composition polycrystalline samples of $Co_{1-x}Mn_xCl_2 \cdot 2H_2O$.

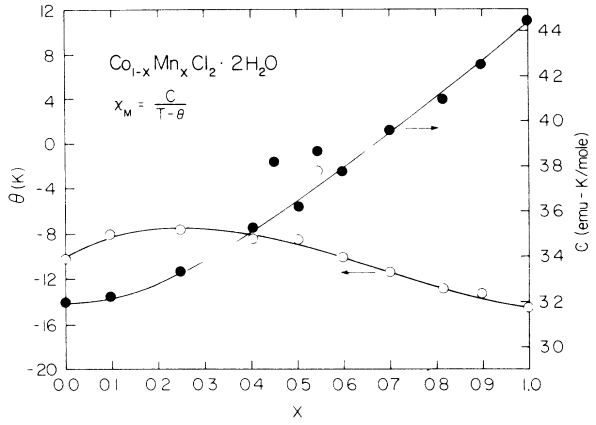

FIG. 3. Curie constant and Weiss Θ vs composition for polycrystalline $Co_{1-x}Mn_xCl_2 \cdot 2H_2O$. Curves through data are only guides to the eye.

$MnCl_2 \cdot 2H_2O$ at the extremes of the diagram, Fig. 3. The variation of Θ with composition in Fig. 3 is also fairly regular, and rather small. From the Mn side ($x=1$), Θ gradually increases with decreasing x until about $x=0.5$, where Θ becomes almost independent of x. For two mixtures, $x=0.452$ and $x=0.545$, Curie constants were 4–6 % larger than expected based on results for the other mixtures; the associated Θ values were also unusually large.

The susceptibilities are shown in more detail for temperatures below 20 K in Figs. 4 and 5. Close examination of the original plots, on which additional data points appear, leads to the assignment of transition temperatures indicated by the arrows. Two arrows are shown for each mixture, one at higher and one at lower temperature. Regarding the former, it is assumed that at a temperature slightly below the maximum which occurs in several mixtures, or in the region of the evident plateau in several others, a transition to an essentially antiferromagnetic

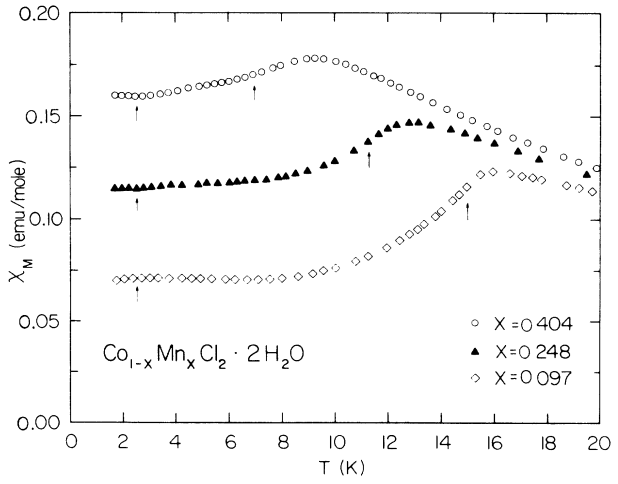

FIG. 4. Susceptibility vs temperature for three cobalt-rich polycrystalline samples of $Co_{1-x}Mn_xCl_2 \cdot 2H_2O$. Arrows indicate estimated transition temperatures as described in the text.

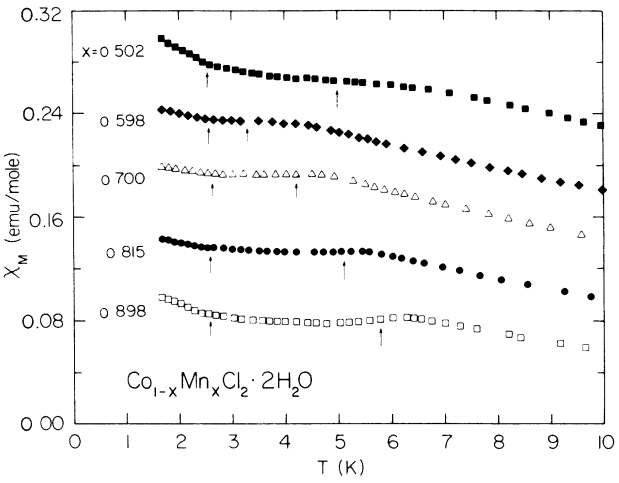

FIG. 5. Susceptibility vs temperature for five manganese-rich polycrystalline samples of $Co_{1-x}Mn_xCl_2 \cdot 2H_2O$. For clarity the susceptibilities of $x=0.502$, 0.700, 0.815, and 0.898 have been shifted +0.04, −0.04, −0.08, and −0.12 emu/mole, respectively. Arrows indicate estimated transition temperatures as described in text.

state occurs. Where possible, the criterion is applied that this upper transition occurs at a temperature where $\partial\chi/\partial T$ is a maximum.[14] This T_u is strongly dependent on composition. In contrast, the position of the lower temperature transition apparent in $\chi(T)$ for each mixture is virtually independent of composition, $T_l = 2.50 \pm 0.10$ K. The anomaly in the susceptibility is often more subtle in this case than for T_u, but appears very clearly on expanded scale plots of the below 4 K region for each mixture (Figs. 6 and 7). Its form is not identical in different mixtures, arguing against the possibilities of either im-

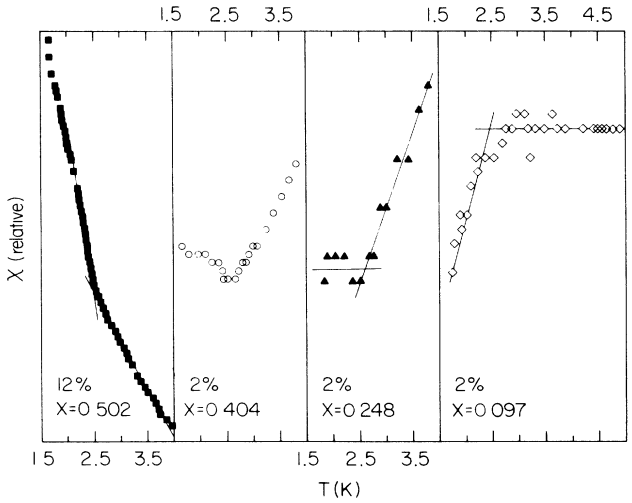

FIG. 6. Expanded scale susceptibility vs temperature plots in the region of the lower transition for several polycrystalline samples of $Co_{1-x}Mn_xCl_2 \cdot 2H_2O$. The total fractional variation (%) over the susceptibility data shown for each composition is also indicated.

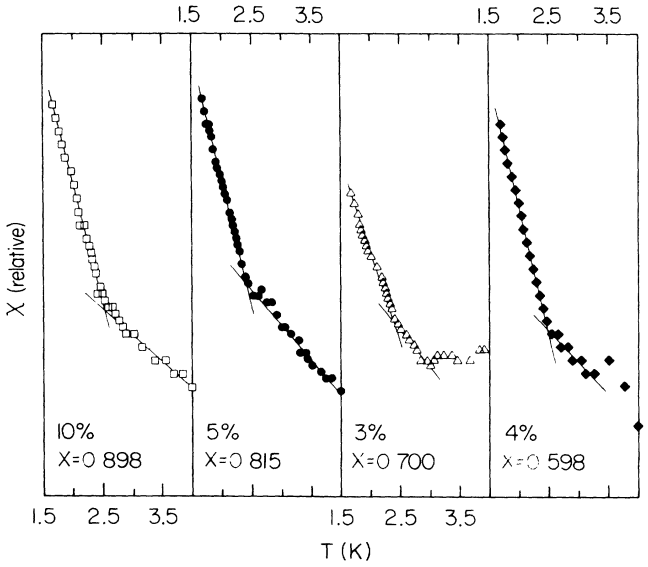

FIG. 7. Expanded scale susceptibility vs temperature plots in the region of the lower transition for several polycrystalline samples of $Co_{1-x}Mn_xCl_2 \cdot 2H_2O$. The total fractional variation (%) over the susceptibility data shown for each composition is also indicated.

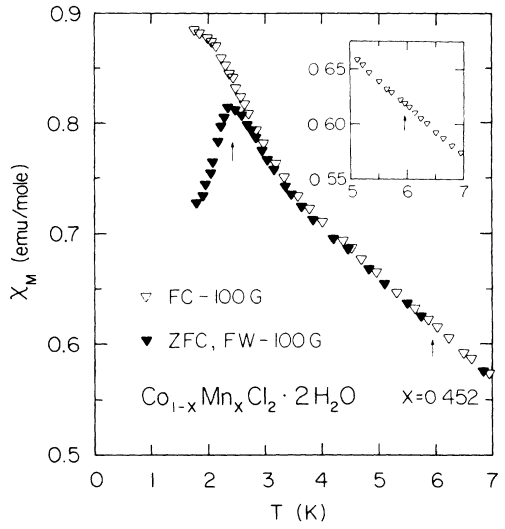

FIG. 8. Field-cooled (FC) and zero-field-cooled (ZFC) or field-warmed (FW) susceptibilities for an $x=0.452$ polycrystalline sample of $Co_{1-x}Mn_xCl_2 \cdot 2H_2O$. Inset shows detail of higher temperature transition near 6 K. Lower temperature arrow indicates maximum in ZFC susceptibility and corresponding lower temperature anomaly in FC susceptibility.

purities or instrumental effects. Moreover, among potential impurities, such as different hydrates of either starting material, only $CoCl_2 \cdot 6H_2O$ has a transition temperature at all similar to T_l, at 2.29 K and significantly lower.[15] Nor is the lower transition less pronounced in Mn-rich mixtures as might be expected if this explanation were correct. A purely instrumental anomaly near T_l was checked for and not found.

Strong evidence in favor of the intrinsic nature of the lower transition is provided by a comparison of field-cooled and zero-field-cooled susceptibilities for an $x=0.452$ sample, in which hysteresis and time-dependent effects (to be discussed) were particularly marked. The data appear in Fig. 8. The higher temperature transition, at $T_u=5.95$ K, was not as obvious as in several other samples, but still observable (inset of Fig. 8). The susceptibility of this sample is unusually large, possibly reflecting an especially high concentration of small paramagnetic clusters or even free spins. Most striking in the data is the pronounced difference between field-cooled and zero-field-cooled susceptibilities, with a rather sharp maximum in the latter at about 2.4_0 K. An anomaly in the field-cooled susceptibility is also discernible at this temperature. A substantial separation between the two susceptibilities is especially evident at all temperatures below about 2.5_0 K. Such behavior is a well-established indication of the existence of a spin-glass phase, here occurring below about 2.5 K.

The magnetization as a function of field for the $x=0.452$ sample at 1.84 K appears in Fig. 9. Rather pronounced curvature is evident above 5 kG, and curvature is also apparent at much lower fields when the field scale is expanded. This behavior will be taken up again in the next paragraph. Also evident in Fig. 9 is significant hysteresis in the magnetization on decreasing the applied field from the 14-kG peak value. The hysteresis is observed to decrease dramatically as the temperature is increased; this is shown in Fig. 10. At or above 2.89 K the fractional hysteresis is 1% or less, but is more than 5% at 2.40 K and more than 70% at 1.84 K. Although the amount of hysteresis is substantially less in other samples, its dependence on temperature is quite similar to that for $x=0.452$ shown in Fig. 10. In general, slight hysteresis is present even above T_u, but is distinctly larger between T_u and T_l, and quite large below T_l. In Fig. 11 the concentration dependence of the hysteresis is displayed. It is much stronger in the region between $x=0.45$ and $x=0.60$ than elsewhere.

Rather similar curvature in $M(H)$, shown for 1.84 K in Fig. 9, was apparent in each of a series of higher tem-

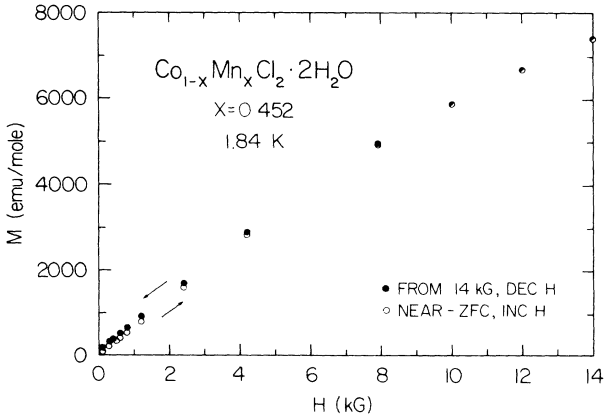

FIG. 9. Magnetization vs field for an $x=0.452$ polycrystalline sample of $Co_{1-x}Mn_xCl_2 \cdot 2H_2O$ at 1.84 K, with hysteresis evident.

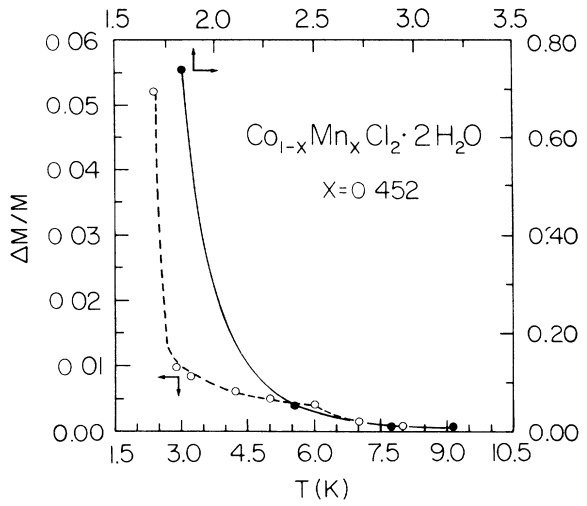

FIG. 10. Temperature dependence of the hysteresis in an $x=0.452$ polycrystalline sample of $Co_{1-x}Mn_xCl_2\cdot 2H_2O$. $\Delta M/M$ is at 200 G, with ΔM taken between values on increasing the field from near zero to 200 G, and on decreasing the field from 14 kG to 200 G. Curves through data are only guides to the eye.

perature isotherms. Each isotherm was analyzed to extract the nonlinear susceptibility, defined as

$$\chi_{NL}(H,T)=\chi_0(T)-M(H,T)/H \ , \tag{1}$$

where $\chi_0=\lim_{H\to 0}(M/H)$ is deduced from the low field portion of each magnetization curve. That is, the magnetization is taken to be expressible as a power series in H, sometimes written in the form[16,17]

$$M=\chi_0 H-b_3(T)(\chi_0 H)^3+b_5(T)(\chi_0 H)^5-\cdots$$
$$=(\chi_0-\chi_{NL})H \ . \tag{2}$$

Figure 12 shows $\chi_{NL}(H,T)$ determined for the $x=0.452$

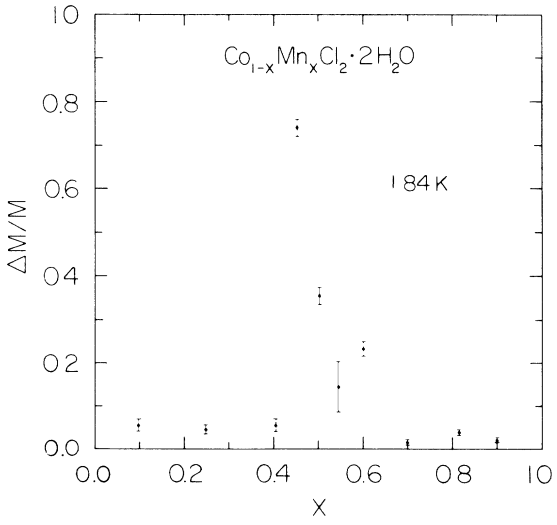

FIG. 11. Concentration dependence of the hysteresis at 1.84 K in various polycrystalline samples of $Co_{1-x}Mn_xCl_x\cdot 2H_2O$. $\Delta M/M$ is obtained as described for Fig. 10.

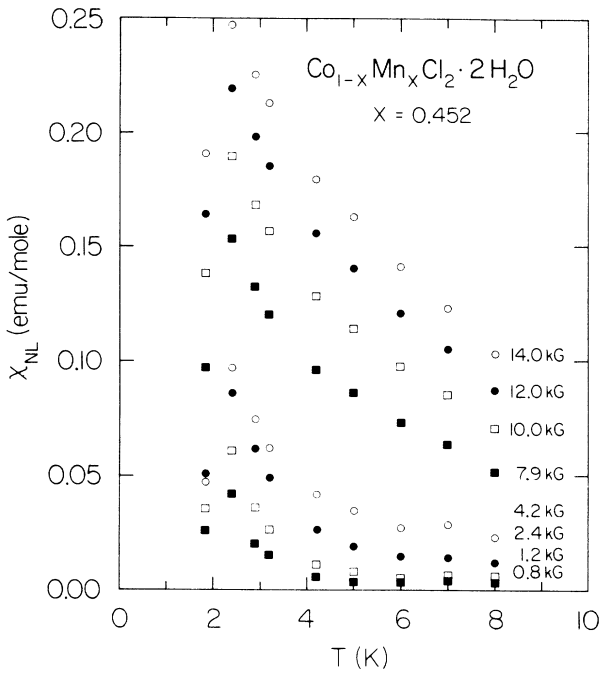

FIG. 12. Nonlinear susceptibility as a function of temperature and field for an $x=0.452$ polycrystalline sample of $Co_{1-x}Mn_xCl_2\cdot 2H_2O$.

sample. It appears that χ_{NL} peaks at a temperature quite similar to the preceding estimates for the spin-glass transition temperature T_g. Its temperature dependence can be further analyzed by examining the behavior of the coefficients b_3 and b_5 in Eq. (2), which can be rearranged to read

$$1-M/\chi_0 H=b_3(T)(\chi_0 H)^2-b_5(T)(\chi_0 H)^4+\cdots \ .$$

Thus a plot of $(1-M/\chi_0 H)/(\chi_0 H)^2$ versus $(\chi_0 H)^2$ will display a zero-field intercept equal to $b_3(T)$ and an initial slope equal to $b_5(T)$.[18] Figure 13 contains such a plot for several temperatures up to about $2T_g$. The derived values of b_3, b_5 are as follows: 0.0242, 0.00501; 0.0324, 0.00923; 0.0770, 0.0413; 0.100, 0.0674; 0.245, 0.312 at 4.997, 4.215, 3.199, 2.894, 2.398 K, respectively, in emu molar dimensions, with b_3 and b_5 estimated to be uncertain by 10% and 20%, respectively, at each temperature. The parameter b_3 increases by one order of magnitude, and b_5 by nearly two orders of magnitude, in this temperature range. Such quasi-divergences in the coefficients are less marked than those observed in the prototypical Ruderman-Kittel-Kasuya-Yosida (RKKY) spin glass Cu-Mn,[17] but are quite similar to recent findings for the insulating spin glass $Fe_{0.3}Mg_{0.7}Cl_2$.[16] From the inset of Fig. 13, constructed for $T_g=2.45$ K, the temperature dependences of b_3 and b_5 appear to be consistent with power laws of the form

$$b_{3,5}\propto[T/(T-T_g)]^{\gamma_{3,5}} \ ,$$

with $\gamma_3=1.22\pm 0.06$ and $\gamma_5=2.20\pm 0.12$. The inset also shows good linearity between $\log_{10}b_5$ and $\log_{10}b_3$, with a

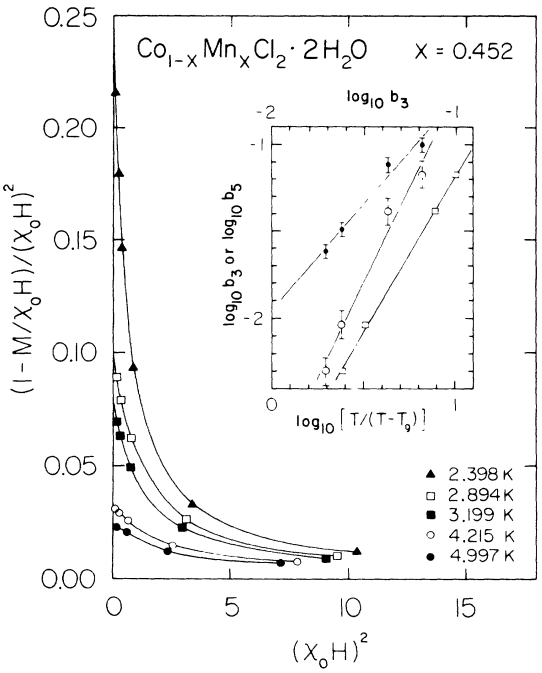

FIG. 13. Analysis of the nonlinear magnetization in an $x=0.452$ polycrystalline sample of $Co_{1-x}Mn_xCl_2\cdot 2H_2O$, according to Eq. (2) as explained in the text. The inset shows the apparent reduced temperature power-law dependences of b_3 (●) and b_5 (○), assuming $T_g=2.45$ K; and also the linearity of $\log_{10}b_5$ in $\log_{10}b_3$ (□).

slope of 1.80 agreeing with $\gamma_5/\gamma_3=1.80$. Analogous behavior has been reported for Cu-Mn.[17] As in Ref. 17, we have employed the nonlinear variable $(T-T_g)/T$ in place of the usual $(T-T_g)/T_g$ in order to extend the range of validity of the simple power-law expression, to temperatures around $2T_g$.

B. TRM and IRM

Two frequently measured properties of spin glasses are the thermoremanent magnetization (TRM) and the isothermal remanent magnetization (IRM).[19] The former is obtained by applying a field above any spin-glass transition, at T_g, cooling the sample to a temperature below T_g, then turning the field to zero and observing the remanent magnetization, generally a decaying quantity. The latter is obtained by cooling the sample in zero field to a temperature below T_g, increasing the field to a desired value, holding it there for a certain period of time (sometimes called the "acquisition time"), then turning the field to zero and observing the remanent magnetization, which will generally decay. Results of TRM and IRM measurements for the $x=0.452$ sample, using various applied fields, appear in Figs. 14 and 15. The maximum in $M_{\rm TRM}(H)$ in Fig. 14 is a typical feature of spin glasses. The position of the maximum in Fig. 14 is seen to shift to slightly lower fields as the measurement time increases, as seen in Cu-Mn,[20] and in $Eu_{0.4}Sr_{0.6}S$.[21] Saturation is approached at a field a few times that of the

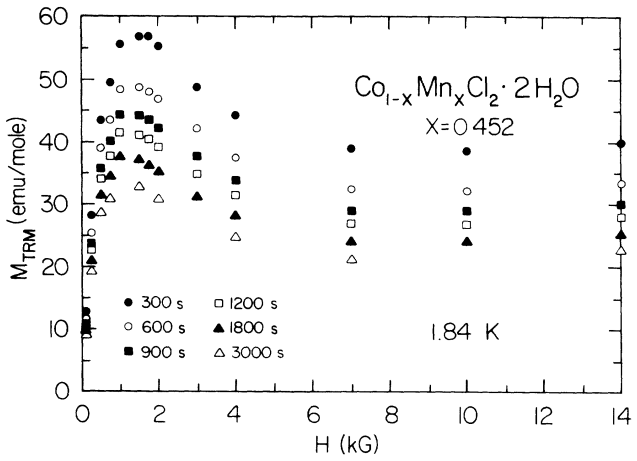

FIG. 14. Thermoremanent magnetization (TRM) as a function of cooling field and measuring time (after turning off field) for an $x=0.452$ polycrystalline sample of $Co_{1-x}Mn_xCl_2\cdot 2H_2O$ at 1.84 K.

maximum, also a typical result, and less than the field required to saturate the (normal) magnetization. Also, though the effect is not large because the times in Fig. 14 span only one decade, the maximum in TRM becomes more pronounced [larger $M_{\rm TRM}(\max)/M_{\rm TRM}(14\text{ kG})$] for longer measuring times. This has also been observed in the most thoroughly studied insulating spin glass, Eu_xSr_{1-x}.[21] Theoretical work has accounted for many of these typical features of the TRM.[22,23] Somewhat less typical is the presence of a weak maximum in $M_{\rm IRM}(H)$ in Fig. 15, occurring at a somewhat higher field than the maximum in TRM. Such a feature has, however, appeared in two theoretical simulations,[22,24] also in measurements on the insulating spin glass $ZnCr_{1.6}Ga_{0.4}O_4$,[6] and most recently in very detailed studies of field dependences in a Cu-Mn spin glass.[20] As expected, the IRM we observe is somewhat less than the TRM for a given

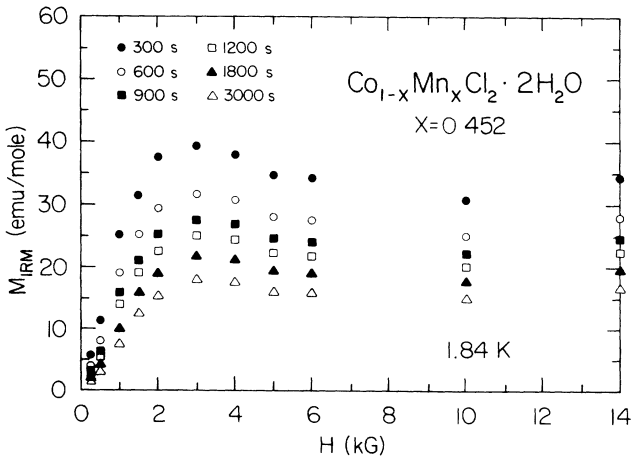

FIG. 15. Isothermal remanent magnetization (IRM) as a function of applied field after zero-field cooling and measuring time (after turning off field) for an $x=0.452$ polycrystalline sample of $Co_{1-x}Mn_xCl_2\cdot 2H_2O$ at 1.84 K.

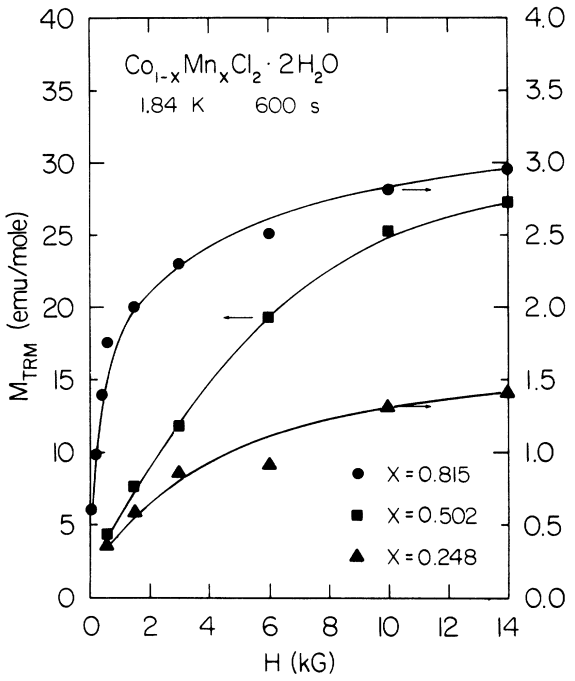

FIG. 16. Thermoremanent magnetization (TRM) as a function of cooling field, 600 s after turning off field, for several polycrystalline samples of $Co_{1-x}Mn_xCl_2 \cdot 2H_2O$ at 1.84 K. Curves through data are only guides to the eye.

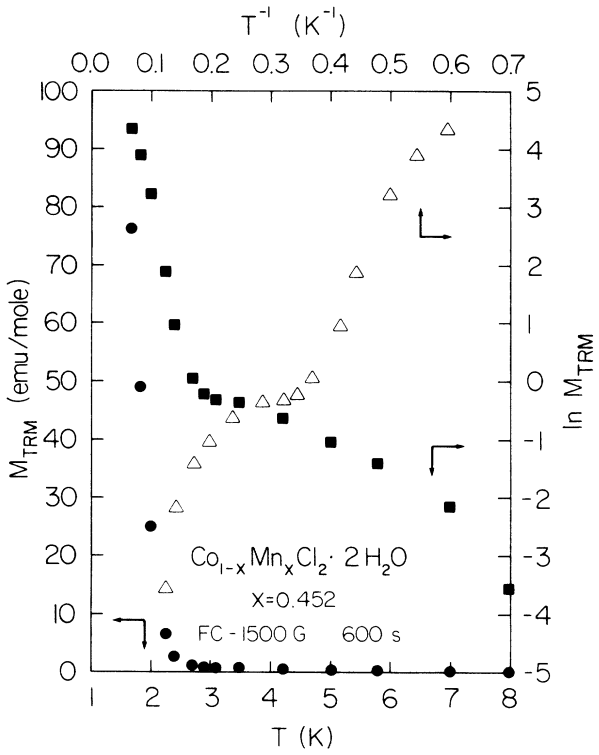

FIG. 17. Temperature dependence of the thermoremanent magnetization (TRM) for an $x=0.452$ polycrystalline sample of $Co_{1-x}Mn_xCl_2 \cdot 2H_2O$, after cooling in a 1500-G field and measuring 600 s after turning off field. TRM vs T (●); ln TRM vs T (■); ln TRM vs $1/T$ (△) are shown.

field and measuring time, and this is so even at 14 kG. At sufficiently high field the saturation values of the two remanences are typically very similar. While not very pronounced, the characteristic S shape of $M_{IRM}(H)$ curves at low field is also evident in the data of Fig. 15. The low field form of the $M_{TRM}(H)$ curve is nonlinear, in agreement with recent findings in the case of Cu-Mn.[20]

The results for some other samples appear in Fig. 16. The TRM is much smaller for $x=0.248$ and $x=0.815$ than for $x=0.502$, which is, however, also smaller than for $x=0.452$. Thus, the concentration dependence of the TRM is somewhat similar to that of the hysteresis discussed earlier, i.e., much smaller when either species is a distinctly minor component. Interestingly, in each of these samples a maximum in $M_{TRM}(H)$ is absent below 14 kG, unlike the case of $x=0.452$. Either only a rather weak maximum occurs at yet higher fields or a gradual approach to saturation occurs. The latter type of behavior seems to have been observed previously in Ni-Mn.[25]

1. Temperature dependence

The temperature dependence of the TRM in the $x=0.452$ sample is shown in Fig. 17. When displayed as simply TRM versus T it is evident that a dramatic increase sets in around 2.7 K, near the temperature T_l identified earlier in susceptibility data. A less marked but still significant enhancement in the TRM occurs below about 6 K, which is approximately T_u in this sample. There is also a small TRM apparent even in the "paramagnetic" region above the upper transition temperature. As a check on the possibility of an activation process for the growth of the TRM, a plot of $\ln M_{TRM}$ versus $1/T$ was made. As is apparent from this representation of the data in Fig. 17, $M_{TRM} \propto \exp(T^*/T)$, with T^* some characteristic temperature, is an inadequate description of the temperature dependence. In some insulating spin glasses an exponential dependence of the TRM on temperature has been observed, $M_{TRM} \propto \exp(-\beta T)$, though typically over a limited temperature range.[4,6] In Fig. 17 the plot of $\ln M_{TRM}$ versus T exhibits a dramatic increase in the TRM below about 2.7 K. The plot is nearly linear in the region 1.65–2.70 K, with some curvature evident at the lowest temperatures which is similar to that observed in $Eu_{0.4}Sr_{0.6}S$.[4] The existence of two temperature regimes can almost be inferred, somewhat as occurred in the insulating spin glass $ZnCr_{1.6}Ga_{0.4}O_4$.[6] However, our data above 2.70 K do not conform nearly so well to a linear relationship as do those of $ZnCr_{1.6}Ga_{0.4}O_4$ above its freezing temperature of 2.40 K. For a cooling field similar (2.0 kG) to that used here, the slope of the $T<T_f$ data for $ZnCr_{1.6}Ga_{0.4}O_4$ was $\beta=1.64$ K^{-1}. For our data below 2.7 K the slope is 5.1 K^{-1}.

2. Time dependence

The time dependence of the TRM in the $x=0.452$ sample is shown in Fig. 18. The rather slow ("viscous") decay extending over a large time interval is a common

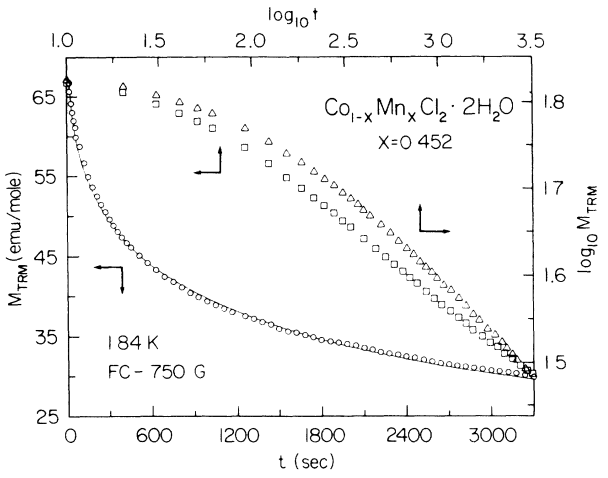

FIG. 18. Time dependence of the thermoremanent magnetization (TRM) for an $x=0.452$ polycrystalline sample of $Co_{1-x}Mn_xCl_2 \cdot 2H_2O$ at 1.84 K, after field cooling in 750 G. TRM vs T (○); TRM vs $\log_{10}t$ (□); $\log_{10}$ TRM vs $\log_{10}t$ (△). Curve through data is a fit described in text.

feature of spin glasses. The exact form of the time dependence has been a matter of controversy for some time, different behavior having been reported for different spin glasses. Thus, both an algebraic time dependence,[6,21] $M(t)=M_0t^{-\alpha}$, and a logarithmic time dependenc,[26,8] $M(t)=M_0-S\log_{10}(t)$, have been reported. The former has also emerged from Monte Carlo simulations[22] as well as from the Sherrington-Kirkpatrick mean-field model of the infinite range Ising spin glass.[27] The logarithmic form can be obtained on the basis of a Néel cluster model taking into account the existence of a wide distribution of blocking temperatures (or relaxation times).[26] The alternative representations of the decay appearing in Fig. 18, $\log_{10}M_{\rm TRM}$ versus $\log_{10}(t)$ and $M_{\rm TRM}$ versus $\log_{10}(t)$, are each quite nonlinear, demonstrating that neither of these forms is an adequate description of the time dependence in the present system, at any rate not over an extended time interval.

In some recent work on examples of both metallic and insulating spin glasses the time dependence of the TRM has been satisfactorily fit using a "stretched" exponential form

$$M(t)=M_0\exp[-C(\omega t)^{1-n}/(1-n)]\ , \tag{3}$$

where C and n are constants and where ω is a relaxation frequency. This form has been derived by Ngai[28] on the basis of a cooperative relaxation model applicable to a variety of disordered systems, including spin glasses. The constant C is predicted theoretically to equal 0.5616. . . . An essentially equivalent and simpler looking stretched exponential decay can also be written,

$$M(t)=M_0\exp[-(t/\tau)^{1-n}]\ , \tag{4}$$

where τ is a characteristic relaxation time. The connecting relation is

$$\tau=\omega^{-1}[C/(1-n)]^{1/(n-1)}\ .$$

Some recent numerical calculations of random-walk diffusion also support a stretched exponential decay, with $n=\frac{2}{3}$;[29] the stretched exponential form has also been obtained in other theories.[30,31]

We have applied the stretched exponential form to the decay of the TRM in the $x=0.452$ sample, at 1.84 K (about the lowest temperature which can be held constant for long periods of time in our apparatus) and for a range of cooling fields from 100 G to 14 kG. For each cooling field the decay can be reasonably well accounted for by the stretched exponential, and certainly much better than by algebraic or logarithmic decay laws. The fit represented by the curve through the data, TRM versus t, in Fig. 18 is typical, with an rms deviation of 0.75% over the fitted range 30–3300 s. The constant C in Eq. (3) has been fixed at 0.562. The relaxation frequency is found to be $\omega=1.95\times10^{-5}$ s^{-1}, for which the equivalent relaxation time in Eq. (4) is $\tau=2190$ s. The fitted value $n=0.74_7$ is similar to values observed in such spin-glass systems as Cu-Mn and Ag-Mn (metallic)[32] and $Eu_xSr_{1-x}S$ and $Eu_xSr_{1-x}Te$ (insulating).[33,34]

The best value of n can be estimated independently, however, from a plot of $\log_{10}[-d(\log_{10}M)/dt]$ versus $\log_{10}(t)$, for which the slope is $-n$ if Eq. (3) or (4) is valid.[35] Figure 19 is such a plot for the data in Fig. 18. The observations $M(t)$ were first fitted with a cubic spline before taking derivatives. It is evident that the resulting plot is not satisfactorily linear, though the slope of a best though poorly fitting line through the data is -0.719 ± 0.016, so that n is near the result obtained previously. Figure 19 suggests, therefore, that the functional form, Eq. (3) or (4), is not quite adequate to describe the decay. There was some indication of this in Fig. 18 as well. Although the rms deviation of the fit is good, careful inspection of the plot reveals that the fitted curve crosses the data in several places (with calculated TRM less than observed between 100 and 400 s, greater than observed between 700 and 1800 s, and less then observed for times above 2400 s), suggesting that the stretched exponential form is only approximate. Such a conclusion has been reiterated in several recent publications of Lundgren and co-workers;[36–38] important insights and

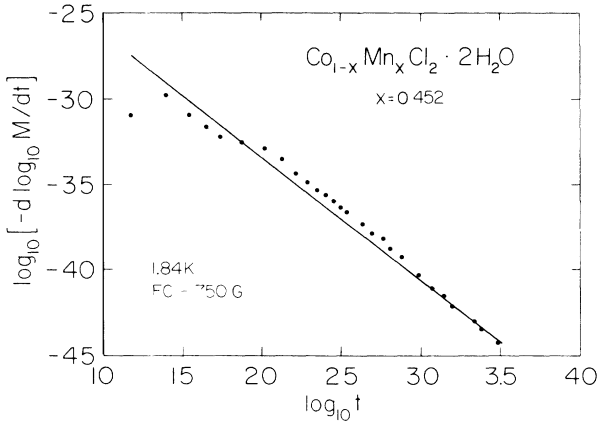

FIG. 19. $\log_{10}$-$\log_{10}$ plot of $-d\log_{10}M/dt$ as a function of time for the data of Fig. 18.

distinctions have also been emphasized by Orbach and colleagues.[39]

Plots of the type of Fig. 18 were constructed for each cooling field, and indicated in each case that the decay of the TRM is neither algebraic nor logarithmic over any extended time interval. Plots of $\log_{10}[-d(\log_{10}M)/dt]$ versus $\log_{10}(t)$ were similar in appearance to Fig. 19 for each field. The slopes ($-n$) of best, though poorly fitting, lines through the data display only a rather unsystematic dependence on field, with only a slight tendency toward larger n values at the highest fields. Except for 14 kG, for which $n=0.90$, all n values were between 0.71 and 0.85. From the $\log_{10}(t)=0$ intercepts the values of ω were also obtained (with $C=0.562$ fixed as previously described). Values ranged from 6.4×10^{-7} s^{-1} to 7.3×10^{-5} s^{-1}, and displayed a somewhat irregular increase with cooling field up to about 3000 G, beyond which a somewhat irregular decrease in ω with increasing field was apparent. Fits to the same data sets employing Eq. (3), with $C=0.562$ fixed and n fixed at values determined from plots of the type of Fig. 19 for each field, yielded ω values similar to those obtained from plot intercepts. M_0 values exhibited a somewhat irregular increase with field.

Since the variation in n with field is not systematic, and the uncertainty in each slope is substantial, the prospect that a more regular trend in ω might emerge if n were held fixed at an approximate mean value among those obtained from plots of the type of Fig. 19 was explored. An n that is essentially independent of field, for $0.2T_g < T < 0.9T_g$ and for low fields, has also been reported for some dilute metallic spin glasses.[32] Fits based on Eq. (3) with $C=0.562$ and $n=0.76$ held fixed yielded values of M_0 and ω shown in Fig. 20. The variation of M_0 with H is less strong than linear in the region below 1 kG; the overall shape of the curve is similar to that of $M_{\rm TRM}(H)$ in Fig. 14. A general increase of ω with field is also apparent, though for fields larger than 2 kG the dependence is much less strong and more irregular. In some recent work on dilute metallic spin glasses a strong field dependence of the apparent relaxation rate ($\propto\omega$) was observed, though it was one which became much weaker as T decreased from $0.98T_g$ to $0.91T_g$.[32] The variation we observe is clear but far weaker; this is probably attributable to our much lower reduced temperature (0.72). However, the fact that the data of Ref. 32 span only the low field range between 5 and 30 G makes detailed comparison with our results difficult.

It is remarkable that despite the very large range of cooling fields employed in this work (100 G to 14 kG), the use of Eq. (3) to fit the TRM decay is nearly equally successful in each case. rms deviations are in the 0.4–1.2% range when n is allowed to vary in the fit, and exhibit a somewhat irregular tendency to increase with cooling field; rms deviations are typically about twice as large when $n=0.76$ is held fixed. The deviations of the fitted curve from the data are also consistently the same for each cooling field, i.e., as remarked earlier in connection with Fig. 18. This is perhaps slightly surprising in light of the frequently stressed view[20,37,38,40] that the form of the time dependence should depend strongly on the magnitude of the cooling field, because (it has been

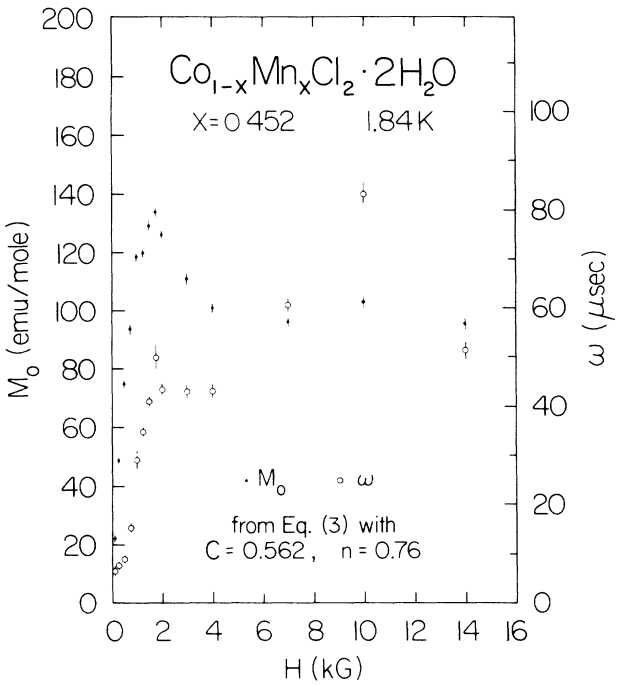

FIG. 20. M_0 and ω vs cooling field for an $x=0.452$ polycrystalline sample of $Co_{1-x}Mn_xCl_2\cdot 2H_2O$ at 1.84 K, from fits to TRM decay data according to Eq. (3) with $C=0.562$ and $n=0.76$ held fixed.

argued) for low fields the effects of aging, which are held to be responsible for the stretched exponential form of relaxation by Lundgren *et al.*,[36,40] are dominating. However, it is likely, based on experience with other materials (e.g., Ref. 33), that for the fields employed here aging effects are strongly suppressed. For the data discussed in the foregoing, the waiting time at the measurement temperature of 1.84 K (before the field was turned off) was well under a minute. No waiting time dependence (for $t_{\rm wait}$ from 1 to 15 min) of the TRM decay was apparent for a 1500-G cooling field.

Other functional forms for the time dependence have also been proposed. Ogielski[41] has performed very large lattice simulations for a short-range Ising spin-glass model in zero external magnetic field and obtained a form

$$q(t)=At^{-a}\exp[-(t/\tau')^b] \tag{5}$$

for the dynamic correlation function, and which should also apply for the thermoremanent magnetization. Equation (5) applies both below and somewhat above the spin-glass transition (short-range correlations grow as T_g is approached from above). Below T_g only the power-law behavior, At^{-a}, could be observed in the simulations. As already noted, from Fig. 18, our data do not conform to a simple power law (algebraic decay). This was confirmed by plotting $\log_{10}(-dM/dt)$ versus $\log_{10}(t)$, which should be linear with slope $-(a+1)$ if the decay is algebraic; this procedure eliminates the effect of potential uncertainties in the zero level remanence. The resulting plot was clearly nonlinear. Therefore Eq. (5), the product of a power law and a stretched exponential, was tried.

Ogielski's results suggest that at T_g b has decreased (from 1 at high temperatures, for normal exponential decay) to a value around 0.35 and a to about 0.06. Both exponents probably decrease further with decreasing temperature. On the other hand, Lundgren *et al.* have argued that a ratio b/a greater than 4 is inconsistent with all of their data, and may be unphysical.[37] We have tried fitting data with a and b fixed at 0.06 and 0.35, respectively; alternatively, with $a=0.06$ and $b=0.24$ fixed, so that b/a is not greater than 4; also with $a=0.025$ and $b=0.31$ fixed, values extrapolated from $a(T)$ and $b(T)$ presented in Ref. 41; and finally with a and b allowed to vary in the fitting procedure.

Taking the last case first, the results did not appear promising. Although very good fits were obtained with two additional parameters varying, with rms deviations of 1.1% or less, the values of a and b did not vary systematically with field. a tended toward values between 0.032 and 0.058 and b toward values between 0.109 and 0.198, so that b especially is smaller than predicted theoretically. Also, the values of τ' displayed no regular dependence on field, but rather varied unsystematically within a range 370–4820 s.

Fits with $a=0.06$ and $b=0.24$ fixed were good, with rms deviations of 1.2% or less. The dependence of τ' on H was a regular decrease up to 1750 G, above which field τ' fluctuated by 10–20 % about its 1750-G value of 2033 s. A increased regularly with field up to 1750 G, above which it decreased slightly and then remained approximately constant. Neither $\log_{10}\tau'^{-1}$ versus H nor $\log_{10}\tau'^{-1}$ versus H^2 appeared linear when plotted. The latter relationship was observed recently in the insulating spin glass $CdIn_{0.3}Cr_{1.7}S_4$, for fields up to 50 G.[42]

Fits with $a=0.025$ and $b=0.31$ fixed were fair, with rms deviations of 1.8% or less. A somewhat more systematic deviation of calculated from observed values was apparent for intermediate times than in the $a=0.06$, $b=0.24$ fits. The variation of A and τ' with field was similar, however, with $\log_{10}\tau'^{-1}$ not linear in either H or H^2.

Fits obtained with $a=0.06$ and $b=0.35$ fixed were comparable in quality with those for $a=0.06$, $b=0.24$, and trends in A and τ' with H were roughly similar. But the linearity of $\log_{10}\tau'^{-1}$ with H^2 was much better than for any of the other sets of a and b, though extending only up to $H=1000$ G. The results are shown in Fig. 21. Although it is not possible to distinguish among the alternatives conclusively, it appears that the form, Eq. (5), is slightly better in accounting for the data than the stretched exponential, Eq. (3), and that the values of the exponents a and b are close to those found in Ref. 41 for temperatures near T_g. However, both the quality of the fit and the pattern of crossings of the data points by the fitted curve, Eq. (5), is very similar to that obtained with the stretched exponential, the example in Fig. 18 being typical.

Most recently Fisher and Huse have predicted, based on a droplet excitation model for the ordered phase of short-range Ising spin glasses, a new form for the decay of the thermoremanent magnetization, which at fixed temperature is[43]

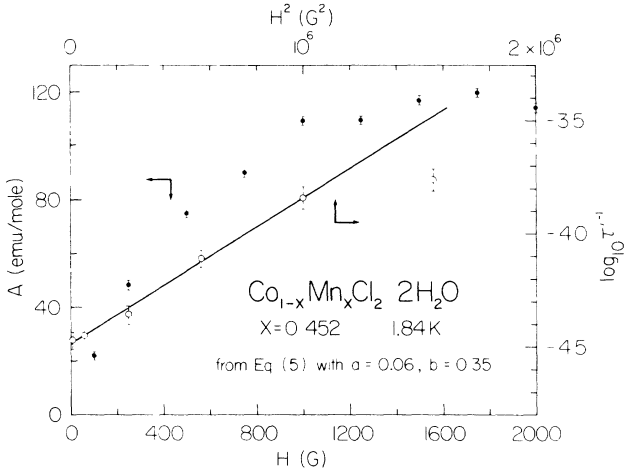

FIG. 21. A (●) vs cooling field H, and $\log_{10}\tau'^{-1}$ (○) vs H^2, for an $x=0.452$ polycrystalline sample of $Co_{1-x}Mn_xCl_2\cdot 2H_2O$ at 1.84 K, from fits to TRM decay data according to Eq. (5) with $a=0.06$ and $b=0.35$ held fixed.

$$M(t)=B[\ln(t/t_0)]^{-R}\ , \tag{6}$$

where t_0 is a microscopic time, R is the ratio of two scaling exponents in the theory, and B is a complicated combination of temperature and other parameters. This expression is thought to apply to both the equilibrium regime, usually taken to be that for which the measuring time is much shorter than the wait time, and to the nonequilibrium regime, where the measuring time is much longer than the wait time. Different values of R are expected in the two cases, with a substantially larger value, greater than 1 and perhaps even as large as 10, in the nonequilibrium situation. In the present experiments rather large applied fields have also been employed, and this may also suggest that on field quenching the decay observed is nonequilibrium, at any rate for sufficiently long times.

Attempts to fit our decay data for the TRM with this form met with little success when the entire observational range 30–3300 s was employed. Since Eq. (6) in our application probably holds only for long times, this result seems reasonable. The fitting was then limited to times of 600 s and above. Because of the very strong correlation among the three parameters under these conditions, it was possible to obtain excellent fits, with rms deviations of a few tenths of a percent, using a substantial range of parameter values. The data could be fit very well with R values between 0 and 1. But then, depending on the field and the assumed R, t_0 was found to range from a few seconds to a few hundred seconds. Such would not appear to be consistent with the definition of t_0 as a microscopic time characterizing the lifetime of a droplet excitation.[44] It was found that by assuming R values larger than one, even better fits could be obtained together with a reduction in t_0. As an example, for the 750-G field-cooled data fitted between 600 and 3300 s, the following fits were obtained (R, t_0, rms deviation): (1.00, 14.22 s, 0.54%), (2.75, 4.99×10^{-3} s, 0.34%), (3.5, 1.67×10^{-4} s,

0.32%), (4.25, 5.37×10^{-6} s, 0.30%), (5.0, 1.45×10^{-7} s, 0.29%). The use of yet larger R values produced very slightly better fits. For a given R the value of t_0 was two to three orders of magnitude smaller at 100 G, and one to two orders of magnitude larger at 7000 G, than at 750 G; t_0 increased uniformly with field up to 7000 G, but decreased slightly at 10 and 14 kG. The fact that only R values substantially larger than one are consistent with a t_0 that is physically plausible (in the ns to μs range) suggests that all the data are taken at sufficiently high cooling field to be in the nonequilibrium regime.

However, it can be shown that the decay form Eq. (6) is inherently less satisfactory as a model for the TRM decay we observe than the stretched exponential form Eq. (3) or (4).[44] Using Eq. (4) one evaluates

$$-d\ \ln M/d\ \ln t=(1-n)\tau^{n-1}t^{1-n}\ ,$$

which increases as t increases. Using Eq. (6) one evaluates

$$-d\ \ln M/d\ \ln t=R\,(\ln t-\ln t_0)^{-1}\ ,$$

which decreases as t increases. (For a power-law decay, $M=M_0t^{-\alpha}$, $-d\ \ln M/d\ \ln t$ is simply α, a constant.) Numerical differentiation of our decay data reveals, for each cooling field, an increasing value of $-d\ \ln M/d\ \ln t$ as t increases. Of course, the power law times stretched exponential form Eq. (5) is also consistent with this finding.

3. *Temperature variation of decay parameters*

The temperature dependence of the TRM decay parameters was also examined. Using a cooling field of 1500 G, $M_{\rm TRM}(t)$ was followed for 2700 s at 1.836, 2.000, 2.250, and 2.398 K. The data were analyzed according to Eq. (3) with $C=0.562$ fixed as before. The linearity of $\log_{10}[-d(\log_{10}M)/dt]$ versus $\log_{10}(t)$-type plots was, as previously, not really satisfactory; nevertheless, an effective n value that increased systematically with temperature was evident. Attempts to fit the data to Eq. (3) with these effective n values (0.813, 0.848, 0.911, and 0.950 at 1.836, 2.000, 2.250, and 2.398 K, respectively) were unsatisfactory in that the variation of the resulting M_0 was unphysical, an increasing M_0 with increasing T. However, the uncertainties in the effective n values are substantial. By adopting a set of smaller n values, each within one or two standard deviations of the above values, and the set as a whole exhibiting a temperature dependence similar to the above, acceptable fits (with rms deviations between 1% and 3%) were obtained with the parameters shown in Fig. 22. Thus, by assuming plausible though not optimal effective n values one obtains physically reasonable values of the other two parameters: M_0 versus T extrapolates to a value $M_0=0$ at a temperature of 2.64 K, not much above the value $T_g=2.50$ K estimated from $\chi(T)$ plots; a dependence of $\log_{10}\tau^{-1}$ on T_g/T which is similar to results in some metallic spin glasses.[32] We note that even for fits obtained with other sets of n values, which did not lead to a physically acceptable $M_0(T)$, the dependence of $\log_{10}\tau^{-1}$ on T_g/T was qualitatively similar to that shown in Fig. 22. That is, a

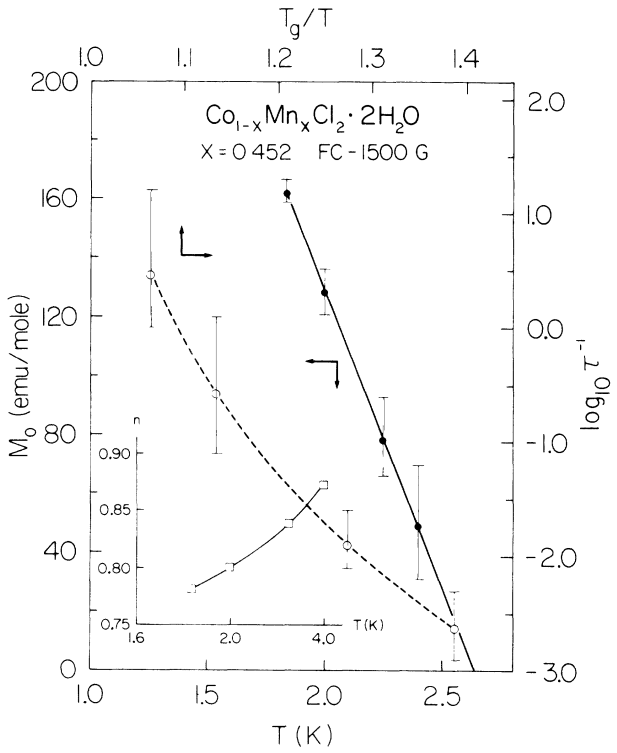

FIG. 22. M_0 (●) and $\log_{10}\tau^{-1}$ (○) as a function of temperature for an $x=0.452$ polycrystalline sample of $Co_{1-x}Mn_xCl_x\cdot 2H_2O$, from fits to TRM decay data for a 1500-G cooling field according to Eq. (4) with $C=0.562$ fixed and with $n(T)$ values (□) shown in the inset.

tendency for τ^{-1} to increase more rapidly than exponentially as T_g is approached from below is evident. Such was also observed in Ref. 32 for T_g/T values between 1.15 and 1.45, the particular range depending on the spin glass. It would appear from Fig. 22 that each of our four temperatures is probably within this faster than exponential regime for the present system.

The decay data at the four temperatures were also analyzed according to Eqs. (5) and (6). a and b in Eq. (5) were fixed at the values 0.06 and 0.35, respectively, which appeared best in earlier fits to 1.836-K data for a range of cooling fields. The results are shown in Fig. 23. A decreases uniformly, but not quite linearly, with increasing temperature, and extrapolates to a zero value at about 2.5 K. Apart from the surprising rise at 2.398 K, τ' decreases with increasing temperature. The variation of τ'^{-1} with T_g/T appears to be slower than exponential, however, in contrast to the behavior found for fits based on Eq. (3). Fits were also performed in which a temperature dependence, suggested by the results in Ref. 41, was imposed on a and b (a varying from 0.025 to 0.06, and b from 0.31 to 0.35, between 1.836 and 2.398 K). rms deviations were slightly larger than before, however, though the variation of A and τ' with temperature was qualitatively very similar.

Fits based on Eq. (6) followed the pattern seen previously for the 1.836-K, variable cooling field decay data; that is, $M_{\rm TRM}(t)$ for $t\geq 600$ could be reproduced to excel-

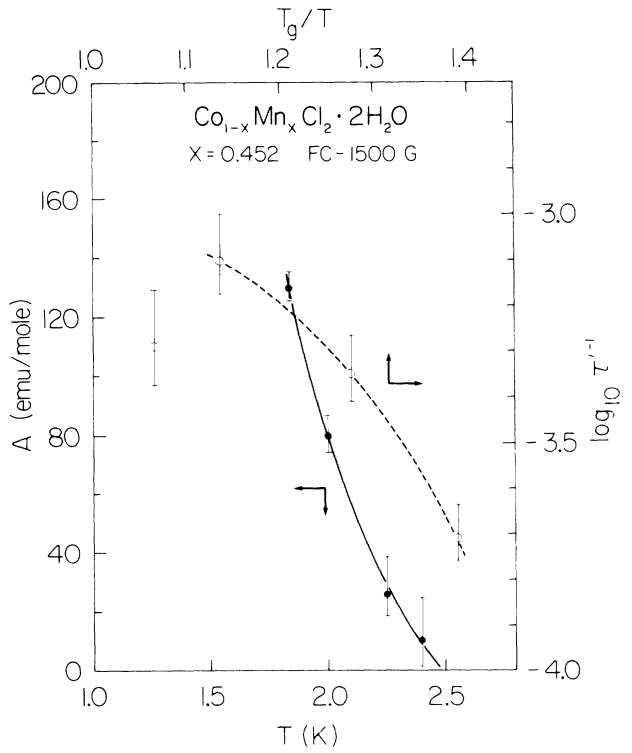

FIG. 23. A (●) and $\log_{10}\tau'^{-1}$ (○) as a function of temperature for an $x=0.452$ polycrystalline sample of $Co_{1-x}Mn_xCl_2 \cdot 2H_2O$, from fits to TRM decay data for a 1500-G cooling field according to Eq. (5) with $a=0.06$ and $b=0.35$ held fixed.

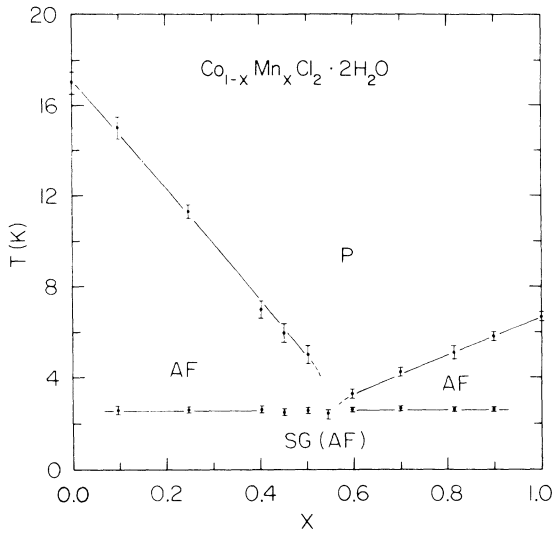

FIG. 24. Magnetic phase diagram of $Co_{1-x}Mn_xCl_2 \cdot 2H_2O$. The region below $T_l=2.5$ K may be a mixed phase with coexistent spin glass and antiferromagnetic order.

lent precision with a wide range of R values, with t_0 (and B) varying accordingly. As for fits based on Eq. (5) discussed in the preceding paragraph, the 2.398-K result appeared anomalous (too small a t_0), but otherwise a strongly increasing t_0 with increasing temperature was observed: for $R=5.00$, $t_0=5.13\times10^{-6}$ s, 1.97×10^{-4} s, 3.28×10^{-3} s at 1.836, 2.000, 2.250 K, respectively. This is as expected. However, for each temperature $-d\ \ln M/d\ \ln t$ is found to increase with increasing t, suggesting that Eq. (6) is inherently less satisfactory than the alternative forms of decay.

IV. DISCUSSION

The magnetic phase diagram constructed from the observed $T_u(x)$ and $T_l(x)$ is shown in Fig. 24. The behavior of the upper phase boundaries is somewhat similar to that observed previously in $Fe_{1-x}Mn_xCl_2 \cdot 2H_2O$,[8] in that $T_u(x)$ decreases from either extreme of the phase diagram. This can be understood as resulting from the increased frustration caused by dissolving either component in the other. Competing orthogonal spin anisotropies as well as competing ferromagnetic and antiferromagnetic exchange interactions occurred in the iron-manganese system, and the phase diagram exhibited a tetracritical point, a second multicritical point, and spin-glass regions. The phase diagram of $Co_{1-x}Mn_xCl_2 \cdot 2H_2O$ is somewhat simpler, but also rather unusual.

The essential constancy of the lower temperature transition, which we identify with the formation of a spin-glass phase, is reminiscent of that found in the mixed ferromagnet-antiferromagnetic $Rb_2Mn_{1-x}Cr_xCl_4$.[5,45] Indeed, the Cr-rich side of the phase diagram of this system is similar to the Co-rich side of Fig. 24, as regards the appearance of $T_u(x)$ and $T_l(x)$. A rather different structure has been reported for the Mn-rich side of $Rb_2Mn_{1-x}Cr_xCl_4$, however,[46] and there seems to be disagreement as to the form of the overall phase diagram as well between Refs. 45 and 46. We note that this mixed system exhibits competing orthogonal anisotropies as well as competing ferromagnetic and antiferromagnetic exchange interactions, and that it is moreover (unlike our system) quasi-two-dimensional. The spin anisotropies are XY-like (Cr) and Heisenberg-like with a small Ising component (Mn), whereas in our system the Co spin is predominantly Ising-like. Another recently examined insulating spin glass is $K_2Cu_xMn_{1-x}F_4$,[47] which is also a mixture of quasi-two-dimensional ferromagnetic and antiferromagnetic ismorphous components with orthogonal spin anisotropies. The phase diagram has ferromagnetic and antiferromagnetic regions at its extremes and an intermediate region ($0.5\leq x\leq0.8$) with a line of paramagnetic–spin-glass transitions, the transition temperature being virtually independent of composition. Such a diagram had been previously conjectured theoretically.[3] Indeed, a number of theoretical treatments have led to the prediction of spin-glass transition temperatures which are virtually independent of composition over a substantial range, e.g., the Sherrington-Kirkpatrick infinite-range Ising model,[27] a Monte Carlo study of two-dimensional XY spin glasses,[48] a Monte Carlo study of a three-dimensional short-range disorder-frustration model,[49] and a study of an Ising spin glass on a Bethe lattice.[50] Most of these models involve short-range interac-

tions. What seems especially interesting about $Co_{1-x}Mn_xCl_2 \cdot 2H_2O$ is that the spin-glass behavior extends over an unusually broad composition range and that it is generally reentrant, except in the near vicinity of $x=0.55$.

However, the possibility that the region below $T_l(x)$ is a mixed state, in which spin glass and antiferromagnetic order coexist, cannot be excluded. Such a state has appeared in the theoretical phase diagram for a three-dimensional frustrated and disordered Ising model.[49] Coexistence of antiferromagnetic and spin-glass states in $Fe_{0.55}Mg_{0.45}Cl_2$ has also been demonstrated and discussed in some detail by Wong *et al.*[51] Since our mixture is three-dimensional and one of its components strongly Ising-like, some of the arguments advanced in Ref. 51 should apply to it as well. Neutron-scattering experiments on $Co_{1-x}Mn_xCl_2 \cdot 2H_2O$ are needed to address this question.

Consideration of the nonlinear susceptibility in Sec. III A supports the idea that a genuine phase transition to a spin-glass state occurs around 2.5 K. The exponents determined in the analysis of Fig. 13, $\gamma_3=1.22\pm0.06$ and $\gamma_5=2.20\pm0.12$, are each somewhat smaller than expected. Although γ_3 (sometimes called[52] γ_s, or simply γ, association with the *non*linear susceptibility being understood) is equal to one in mean-field theory, experimental determinations on a variety of spin glasses, both RKKY and insulating, have generally yielded values between 2 and 4.[17,53–56] It is also expected that[56] $\gamma_5=2\gamma_3+\beta$. In mean-field theory $\beta=1$, but is typically found to be slightly less than 1 in real spin glasses.[17,55–57] Thus, one expects γ_5 to be from 2 to 3 times larger than γ_3, while we find a value not quite twice as large. Apart from the extended temperature range (to $2T_g$) of the analysis, and the limited data, discrepancies in exponent values may originate from the fact that the extrapolation used (Fig. 13) to determine b_3 and b_5 had to be based on somewhat higher field data (≥ 600 G) than are strictly appropriate in connection with asymptotic critical behavior. A scaling analysis of $\chi_{NL}(H,T)$ which provides more information on these and related questions will be published separately.

In Sec. III B 2 Eq. (5) appeared to be the most satisfactory form of those used to model the TRM decay, though only a small improvement over fits using a pure stretched exponential, Eq. (3) or (4), was detectable. In certain other attempts[37,58] to use such an expression the field, temprature, or wait time regimes were different, so that comparisons are difficult to make. The true significance of the stretched exponential decay form remains a matter of controversy. Our relatively large fields suppress waiting time effects [so that t' is presumably long in an expression of the type[59,32] $\tau^{-1}=\omega' \exp(-t_{wait}/t')$ for the wait time dependence of the response time], and yet a stretched exponential consistently emerges from our data analysis. We may be in the short to moderate this regime, as discussed by Hoogerbeets *et al.*,[39] where a pure stretched exponential decay can be anticipated. If the fact that $t \gg t_{wait}$ for our measurements is relevant even though no waiting time dependence was apparent, the presence of a power-law prefactor can perhaps also be rationalized. One interesting aspect of our results, not observed previously so far as we know, is the success in fitting the decay data with the same general forms even for very large cooling fields.

As discussed in Secs. III A and B many samples besides $x=0.452$ exhibited significant hysteretic effects and thermoremanent magnetizations, and all samples exhibited at least small effects of this kind. The TRM in other samples were also time dependent, but because of their smaller size were more difficult to measure precisely and to analyze. Nonlinearities in M versus H were also present, but were usually much smaller than in $x=0.452$, and so we have not attempted to extract the nonlinear susceptibility for these samples. A scaling analysis of the nonlinear susceptibility in the $x=0.545$ mixture will be published separately.

It is presumably not irrelevant that the $x=0.452$ mixture (along with $x=0.545$) exhibited an enhanced Curie constant and Weiss Θ (Fig. 3) relative to the other mixtures. Frustration can be expected to be greater near the center of the diagram, and it is possible that the degree of short-range antiferromagnetic clustering is greater in these two samples than in the others. Cluster formation has been found in theoretical studies[60–62] and has been inferred in some experimental work, especially on insulating spin glasses.[4,6,63,64] It has also been suggested[65] that frustration in systems with predominantly antiferromagnetic interactions can lead to frequent local cancellation of internal fields and to enhanced paramagnetic behavior, as Fig. 3 may be suggesting. It is difficult to be precise about the nature of the clustering in our system, but from work on other materials one can speculate that the gradual freezing of clusters as T_g is approached from above may lead to a more random distribution of internal fields than would otherwise be the case, and thus to enhanced spin-glass behavior. A small amount of chemical clustering might also be a contributing factor, and cannot be ruled out because the sample analysis and characterization techniques employed do not probe at the necessary microscopic level. Still, we tend to favor the preceding explanation in terms of antiferromagnetic clusters. It should be emphasized again that while the spin-glass behavior in $x=0.452$ and $x=0.545$ is particularly strong, the other mixtures also exhibited weaker effects of this kind. The T_l transition is present in each mixture. Therefore we believe that our picture of the overall properties of this interesting new insulating spin glass is correct.

ACKNOWLEDGMENT

This work was supported by National Science Foundation–Solid State Chemistry Grant No. DMR-8511163.

[1]P.-Z. Wong, Phys. Rev. B **34**, 1864 (1986); P.-Z. Wong, P. M. Horn, R. J. Birgeneau, and G. Shirane, *ibid.* **27**, 428 (1983).
[2](a) W. Nitsche and W. Kleeman, J. Magn. Magn. Mater. **54–57**, 37 (1986); Phys. Rev. B **36**, 8587 (1987). (b) B. D. Howes, D. C. Price, and M. C. K. Wiltshire, J. Phys. C **17**, 3669 (1984).
[3]S. Fishman and A. Aharony, Phys. Rev. B **21**, 280 (1980).
[4]H. Maletta and W. Felsch, Phys. Rev. B **20**, 1245 (1979); H. Maletta, J. Appl. Phys. **53**, 2185 (1982), and numerous subsequent papers.
[5]H. Kubo, T. Hamasaki, M. Tanimoto, and K. Katsumata, J. Phys. Soc. Jpn. **55**, 3301 (1986); K. Katsumata, J. Magn. Magn. Mater. **54–57**, 75 (1986).
[6]D. Fiorani, S. Viticoli, J. L. Dormann, J. L. Tholence, and A. P. Murani, Phys. Rev. B **30**, 2776 (1984).
[7]A. Ito, H. Aruga, E. Torikai, M. Kikuchi, Y. Syono, and H. Takei, Phys. Rev. Lett. **57**, 483 (1986); H. Yoshizawa, S. Mitsuda, H. Aruga, and A. Ito, *ibid.* **59**, 2364 (1987).
[8]G. C. DeFotis, C. Pohl, S. A. Pugh, and E. Sinn, J. Chem. Phys. **80**, 2079 (1984).
[9]J. N. McElearney, S. Merchant, and R. L. Carlin, Inorg. Chem. **12**, 906 (1973).
[10]F. Matsubara and S. Inawashiro, J. Phys. Soc. Jpn. **46**, 1740 (1979).
[11]A. Narath, Phys. Rev. **136**, 766 (1964); **140**, 552 (1965).
[12]H. Mollymoto, M. Motokawa, and M. Date, J. Phys. Soc. Jpn. **49**, 108 (1980).
[13]G. C. DeFotis, B. K. Failon, F. V. Wells, and H. H. Wickman, Phys. Rev. B **29**, 3795 (1984); G. C. DeFotis and J. R. Laughlin, J. Chem. Phys. **84**, 3346 (1986).
[14]M. E. Fisher, Philos. Mag. **7**, 1731 (1962).
[15]W. K. Robinson and S. A. Friedberg, Phys. Rev. **117**, 402 (1960).
[16]F. Bensamka, D. Bertrand, A. R. Fert, and J. P. Redoules, J. Phys. C **19**, 4741 (1986).
[17]R. Omari, J. J. Prejean, and J. Souletie, J. Phys. (Paris) **44**, 1069 (1983).
[18]D. Fiorani, J. L. Dormann, J. L. Tholence, L. Bessais, and D. Villers, J. Magn. Magn. Mater. **54–57**, 173 (1986).
[19]J. L. Tholence and R. Tournier, J. Phys. (Paris) **35**, C4 (1974).
[20]P. Nordblad, L. Ludgren, and L. Sandlund, Europhys. Lett. **3**, 235 (1987).
[21]J. Ferre, J. Rajchenback, and H. Maletta, J. Appl. Phys. **52**, 1697 (1981).
[22]W. Kinzel, Phys. Rev. B **19**, 4595 (1979).
[23]A. Aharoni and E. P. Wohlfarth, J. Appl. Phys. **55**, 1664 (1984).
[24]C. M. Soukoulis, K. Levin, and G. S. Grest, Phys. Rev. B **28**, 1495 (1983).
[25]W. Abdul-Razzaq and J. S. Kouvel, J. Appl. Phys. **55**, 1623 (1984).
[26]C. N. Guy, J. Phys. F **7**, 1505 (1977); **8**, 1309 (1978).
[27]D. Sherrington and S. Kirkpatrick, Phys. Rev. Lett. **35**, 1792 (1975).
[28]K. L. Ngai, Commun. Solid State Phys. **9**, 127 (1979).
[29]I. A. Campbell, J. M. Flesselles, R. Jullien, and R. Botet, J. Phys. C **20**, L47 (1987).
[30]R. Rammal, J. Phys. (Paris) **46**, 1837 (1985).
[31]C. De Dominicis, H. Orland, and F. Lainee, J. Phys. (Paris) Lett. **46**, L463 (1985).
[32]R. Hoogerbeets, W.-L. Luo, and R. Orbach, Phys. Rev. B **34**, 1719 (1986).
[33]J. Ferre, M. Ayadi, R. V. Chamberlin, R. Orbach, and N. Bontemps, J. Magn. Magn. Mater. **54-57**, 211 (1986).
[34]F.-J. Börgermann, H. Maletta, and W. Zinn, Phys. Rev. B **35**, 8454 (1987).
[35]R. V. Chamberlin, G. Mozurkewich, and R. Orbach, Phys. Rev. Lett. **52**, 867 (1984).
[36]P. Nordblad, P. Svedlindh, L. Lundgren, and L. Sandlund, Phys. Rev. B **33**, 645 (1986).
[37]L. Lundgren, P. Nordblad, and P. Svedlindh, Phys. Rev. **34**, 8164 (1986).
[38]P. Nordblad, L. Lundgren, P. Svedlindh, L. Sandlund, and P. Granberg, Phys. Rev. B **35**, 7181 (1987).
[39]R. Hoogerbeets, W.-L. Luo, and R. Orbach, Phys. Rev. B **35**, 7185 (1987).
[40]P. Svedlindh, P. Granberg, P. Nordblad, L. Lundgren, and H. S. Chen, Phys. Rev. B **35**, 268 (1987).
[41]A. T. Ogielski, Phys. Rev. B **32**, 7384 (1985).
[42]M. Alba, E. Vincent, J. Hammann, and M. Ocio, J. Appl. Phys. **61**, 4092 (1987).
[43]D. S. Fisher and D. A. Huse, Phys. Rev. Lett. **56**, 1601 (1986); Phys. Rev. B **38**, 373 (1988); **38**, 386 (1988).
[44]We thank Professor Fisher and Dr. Huse for comments on various points.
[45]K. Katsumata, M. Tanimoto, S. Mitsuda, and Y. Endoh, J. Phys. Soc. Jpn. **53**, 3315 (1984).
[46]G. Munninghoff, E. Hellner, W. Treutmann, N. Lehner, and G. Heger, J. Phys. C **17**, 1281 (1984).
[47]Y. Kimishima, H. Ikeda, A. Furukawa, and H. Nagano, J. Phys. Soc. Jpn. **55**, 3574 (1986).
[48]H. Kawamura and M. Tanemura, J. Phys. Soc. Jpn. **55**, 1802 (1986).
[49]H. T. Diep and O. Nagai, J. Phys. C **18**, 369 (1985).
[50]J. M. Carlson, J. T. Chayes, L. Chayes, J. P. Sethna, and D. J. Thouless, Europhys. Lett. **5**, 355 (1988).
[51]P.-Z. Wong, S. von Molar, T. T. M. Palstra, J. A. Mydosh, H. Yoshizawa, S. M. Shapiro, and A. Ito, Phys. Rev. Lett. **55**, 2043 (1985).
[52]M. Suzuki, Prog. Theor. Phys. **58**, 1151 (1977).
[53]B. Barbara, A. P. Malozemoff, and Y. Imry, Phys. Rev. Lett. **47**, 1852 (1981).
[54]E. Zastre, R. M. Roshko, and G. Williams, Phys. Rev. B **32**, 7597 (1985).
[55]P. Svedlindh, L. Lundgren, P. Nordblad, and H. S. Chen, Europhys. Lett. **2**, 805 (1986).
[56]E. Vincent and J. Hammann, J. Phys. C **20**, 2659 (1987).
[57]Y. Yeshurun, L. J. P. Ketelsen, and M. B. Salamon, Phys. Rev. B **32**, 7425 (1985).
[58]M. Alba, M. Ocio, and J. Hammann, Europhys. Lett. **2**, 45 (1986).
[59]R. V. Chamberlin, Phys. Rev. B **30**, 5393 (1984).
[60]A. J. Bray, M. A. Moore, and P. J. Reed, J. Phys. C **11**, 1187 (1978).
[61]R. Rammal, R. Suchail, and R. Maynard, Solid State Commun. **32**, 487 (1979).
[62]A. E. Jacobs, Phys. Rev. B **32**, 7430 (1985).
[63]D. Fiorani, J. L. Dormann, J. L. Tholence, and J. L. Soubeyroux, J. Phys. C **18**, 3053 (1985).
[64]Y. Tazuke, J. Phys. Soc. Jpn. **55**, 2008 (1986).
[65]J. L. Tholence, Y. Yeshurun, and B. Wanklyn, J. Phys. C **19**, 235 (1986).